ORIGINAL ARTICLE

Novel epoxy nanocomposite with nano TiO$_2$ and Al$_2$O$_3$ by D-optimal combined design and partial least squares discriminate analysis for food packaging

Samira Siami Araghi[1], Seyed Mohamad Ali Ebrahimzadeh Mousavi [2,], Ali Akbar Safekordi [3], Reza Dinpanah[1]*

[1] *Department of Food Science and Technology, Sari Branch, Islamic Azad University, Sari, Iran*
[2] *Department of Food Science and Technology, University of Tehran, Iran*
[3] *Professor at Sharif University of Technology, Sharif University of Technology, Tehran, Iran*

Abstract
This study aimed to use D-optimal combined design, and partial least squares discriminate analysis (PLS-DA) to investigate the mechanical properties, and chemical compatibilities of improved epoxy nanocomposites by nano TiO$_2$/Al$_2$O3. Experimental design of adhesion, and wedge bend properties led the results into the optimum values of TiO$_2$= 0.66%, Al$_2$O$_3$= 1.33%, dispersant= 0.000017%. The variable importance of the projection (VIP) score and PLS-DA modeling were used to categorize mechanical properties and chemical compatibilities. The best point could be identified from the other samples, based on the results. PLS-DA could explain 94.32% of the total variance in the data and wedge bend, adhesion and thermal treatment were the most significant variables with VIP scores at 2.73, 2.02, and 1.38, respectively. The morphology was examined using a field emission scanning electron microscope (FESEM). The thermal properties of nanocomposites were described by differential scanning calorimeter (DSC) to define the glass transition temperature for epoxy-nanocomposites. The mechanical properties were measured to assess the storage modulus via the dynamic mechanical analysis (DMA). Epoxy/TiO$_2$/Al$_2$O$_3$ nanocomposite exhibited a uniform particle distribution, as indicated by the FESEM image. Adding nanoparticles significantly raised the glass transition temperature. The presence of nanoparticles can be used to enhance storage modulus functionally.

Keywords: *Chemical Properties; DMA; DSC; FESEM; Mechanical Properties.*

INTRODUCTION

The Epoxy resin is a sort of high-performance thermoset that is widely used in various applications. Epoxy resins are known for their favorable properties like the adhesion that comes from the hydroxyl group, and their chemical resistance is due to the presence of ether bonds, and aromatic rings in their structure, which make them stable against heat and hardness, and the methyl bonds can improve their mechanical properties [1]. Epoxy rings on two of the chain's end sides create a three-dimensional network and a hard layer on the coated surface. By direct copolymerization, epoxy lacquer was created using phenol formaldehyde and melamine resin [2, 3]. The phenol-formaldehyde resin is widely used for coating due to its many advantages, such as good mechanical properties, and heat resistance [4]. Amorphous melamine is an amino resin with various material advantages, such as better hardness, thermal stability, scratch resistance, and surface smoothness, which makes it ideal for use in large industrial applications [5]. These kinds of ingredients have the potential to modify the thermosetting resin, and composition of the hydroxyl groups, and improve

* Corresponding Author Email: *mousaviut52@gmail.com*

performance in epoxy lacquer.

A well-known method to alter the unique features of polymers in recent years is the introduction of nanosized filler into different polymers or epoxies [6-8]. One of the main targets of using nanocomposite is to use the building blocks with nano dimensions to design and create new materials that achieve new properties. Although the high specific surface area of nanoparticles results in intense interfacial contact between the particles and polymer matrix, it induces the formation of micrometer-sized agglomerates and electrostatic attraction among the particles [9]. Nanoparticles must therefore be homogeneously dispersed within the matrix to benefit from the advantages of a high surface area. There are various techniques for infusing the nanoparticles into a polymer, such as melt mixing [10], solution mixing [11], in situ interaction polymerization [12], shear mixing [13], and mechanical stirring [14]. The effort of mixing on the dispersion of nanoparticles in nano epoxy composite was studied in many investigations.

Based on previous studies, with adding nanofillers to polymers, have been leads to improved polymer properties that are different from the properties of conventional polymers [15]. Al-Turaif [16] studied the mechanical properties of epoxy resin with TiO_2 nanoparticle size. The modified epoxy showed improved tensile stress and flexural performance, according to the results. The effects of nanoscale SiO_2, TiO_2, Fe_2O_3, ZnO, and clay on the thermal and mechanical characteristics of the epoxy coating were investigated by Nguyen *et al.* [17]. They found that Fe_2O_3 and nanoscale clay might boost epoxy coating's adhesive strength. Nano SiO_2, nano Fe_2O_3, and nano ZnO enhanced the thermal stability of epoxy, and nano TiO_2 showed the best strength improvement. Jiang *et al.* [18] studied the thermo-mechanical behavior of epoxy nanocomposite with Al_2O_3. Based on their results, nano Al_2O_3 had little effect on the thermal stability of nanocomposites.

The design of the expert method is a statistical tool that reduces the number of experiments necessary for studying the effects of various parameters on the product quantity or quality. This method screens the significant factors affecting the response from the less significant ones, and provides the optimum condition to achieve the most desirable performance [19]. The effect of materials and mixing conditions on the mechanical properties and chemical compatibility of nano epoxy composites has never been studied experimentally, despite some studies in the field. Moreover, little attention has been paid to using different resins for the nanocomposite preparation.

This research aimed to study the effect of nano TiO_2 (A), nano Al_2O_3 (B), and a dispersant (C), two different formulas (E, e) and two different mixing methods (D, d) on the mechanical properties of nano epoxy composite using an experimental design approach. Using Matlab software, the link between mechanical characteristics and chemical compatibilities was investigated. Qualitative responses were classified using PLS-DA based on mechanical characteristics and chemical compatibilities. Finally, under ideal nanoparticle, formula, and mixing mode circumstances, the morphological, thermal, and mechanical characteristics were investigated.

MATERIALS AND METHODS
Materials
Bisphenol A diglycidyl ether (BADGE) epoxy resin EPO-TEK®H20E was provided from Epotek, USA, phenolic mounting resins were purchased from PACE Technologies, USA and carboxylic acid PAF C-16 were purchased from Cayman, USA as curing agents in conjunction with TEGOPERN®6875 were purchased from Evonik, Germany as a dispersant were used. TiO_2 Nanoparticles of a mean diameter of 10-30 nm, and Al_2O_3 Nanoparticles with an average diameter of 20 nm were prepared from US Research Nanomaterials Inc., USA. The purity of TiO_2 and Al_2O_3 was 99.9%.

Methods
Production method of nanocomposite
To prepare the mixture, the phenol-formaldehyde curing agent was added to the epoxy resin with the ratio of 100 : 17 w/w (Donated as E). Carboxylic acid and phenol formaldehyde were added to the epoxy resin with the ratio of 100 : 43 w/w (Donated as e). According to Nguyen *et al.* [20], different quantities of TiO_2 and Al_2O_3 nanoparticles (up to 2%) were added after premixing the mixture and adding the required quantity of dispersant. Two mixing techniques, ultrasound and high-speed mixing were combined to create a homogeneous solution. High-speed mixing was carried out for 15 min at room temperature using an IKA T25 digital Ultra-TURRAX® homogenizer at a speed of 15000 rpm [21]. After degassing the solution, ultrasonic vibration with a maximum output

power of 70 W and a constant frequency of 28 KHz was used. An ultrasonic amplitude of 90% was applied with a pulse (9s on, 1s off) for about 16 min [22]. The mixing breaker was placed in a water bath for external cooling to establish a steady temperature environment. These treatments were applied to flat tin plates that had been coated with the appropriate nanocomposite and heated to 190 °C for 15 minutes.

Nanocomposite mechanical test method

Coated surfaces were examined using the adhesion test, and the outcomes were assessed using a technique that complies with ASTM D3359-09. On the dried film from a metal substrate, the test was conducted using a cross-cut tester. Then, the adhesion of samples was measured (6x-10x magnification), by rubbing and pulling off banderole on the dried film. The specimens were scored from 1 (highest score for samples without any blowing) to 5 (lowest score for samples with extreme blow).

To measure the flexibility of dried film wedge bend test was used (ASTM E23). A Hofer, model HF C300, with a hammer weight of 2300 g and drop height of 650 mm was used. The size of the samples was 140 mm × 70 mm. The samples were observed (original magnification 6X and 10X), and scored by percentage of scratch.

Nanocomposite Chemical compatibility test method

Based on ASTM D543, the chemical compatibility of the nanocomposite was tested. To assess the resistance of coatings to chemical reagents under sterilization and pasteurization conditions, chemical compatibility was established. Lactic acid, chloro-cysteine, citric acid, and acetic acid were all components of the sterilizing solution. Citric acid served as the pasteurization condition's equalized solution. Acetic acid glacial 2%, citric acid 2%, and lactic acid 1.3% were used as chemical reagents. The abovementioned chemicals were prepared from Tosseh Nano Fanavar Kashef, IRAN, and L-cysteine hydrochloride monohydrate 0.5%

was bought from Merck Germany in a completely sterile condition. Then, the mechanical properties of the samples were evaluated (1 point was assigned to the highest quality and 0 to the lowest quality).

Nanocomposite optimization method

The effects of independent variables included TiO_2 (donated as A), Al_2O_3 nanoparticles (donated as B), Tegopern® 6875 (donated as C) as dispersant agents and two mixing methods included ultrasound (donated as d), and ultra-turrax (donated as D), and two formulas included epoxy resin, phenol formaldehyde, and other solvents (donated as E) and epoxy resin, phenol formaldehyde, melamine, and other solvents (donated as e) on adhesion and wedge bend properties of the modified coating were investigated. The test plan was created using the Design-Expert 7.1.5 application. While dispersant was given a numerical type variable classification, $TiO2$ and $Al2O3$ nanoparticles were categorized as mixed type variables. As shown in Table 1, mix and formula were categorized as category type variables. Using the best-fit model, the correlation between independent variables and responses was found. The best-fitted model was selected based on some elements, such as high R-squared, low standard deviation, and significance of the model based on the analysis of variance. The statistical comparisons of predicted values, and actual values of the optimized points were tested by paired t-test using SPSS software (Ver. 22.0, IBM Corp, Armonk, NY, USA). The chemical compatibility results included acetic acid, citric acid, lactic acid, and L-cysteine hydrochloride monohydrate were donated as 0 (not acceptable), and 1 (acceptable). Chemical compatibility results were imported to Matlab and used to build up X block variables (data matrix X). Independent variables were coded and utilized as the y block variables, including mixing and formula. These evaluations were conducted using PLS Toolbox 7.8 and MATLAB R2013a software. The relevance of each variable in the PLS-DA model was categorized in

Table 1. Treatments and coded levels of independent variables.

Variables	Symbols coded	Type	Coded levels		
			-1	0	1
TiO_2 (%)	A	Mixture	0	1	2
Al_2O_3 (%)	B	Mixture	0	1	2
Dispersant (%)	C	Numeric	0	0.005	0.01
Mix	D	Categoric	D	-	d
Formula	E	Categoric	E	-	e

the following using the VIP score as a straightfor-ward strategy tool [23, 24].

Field Emission Scanning Electron Microscope (FE-SEM) study of optimized nanocomposite

The surface morphology and the dispersion state of TiO_2 and Al_2O_3 nanoparticles within the polymeric matrix were studied using FESEM (Mira3 Tescan, Czech) with an energy dispersive Xrays analyzer (EDX) to determine the size, as well as the identity of present particles in the material. The coated steel panels were subjected to the application of a thin layer of a gold coating before carrying out the tests to minimize the charging effects.

Differential Scanning Calorimeter (DSC) study of optimized nanocomposite

Comparative Scanning The glass transition temperature, Tg, which marks the shift from a glassy solid phase to a super-cooled liquid state, was determined using a calorimeter on samples by Mettler Toledo, Switzerland. The range of temperature for prepared nanocomposite, and neat epoxy was done from 30 to 300 °C, at a heating

rate of 10 °C/min according to ASTM D3418 [25].

Dynamic Mechanic Analysis (DMA) study of optimized nanocomposite

Dynamic Mechanic Analysis was performed using a TA Instrument 2980, at three-point bending mode at an oscillation frequency of 1 Hz. Temperature scanning was performed from -60 to 100 °C on a heating rate of 5 °C/min [26]. The final sample specimen shape was performed as 2 mm × 30 mm × 12 mm.

RESULTS AND DISCUSSION
Experiment design of nanocomposite

The experiment design was carried out based on Table 2. Independent variables included TiO_2 nanoparticles, Al_2O_3 nanoparticles, Tegopern® 6875 as dispersant agent, and two mixing methods included ultrasound, and ultra-turrax, and two formulas named E (included epoxy resin, phenol formaldehyde and other solvents), and e (included epoxy resin, phenol formaldehyde, melamine, and other solvents). As shown in Table 2, 34 runs were done based on a D-optimal combined design.

Table 2. D-optimal combined design and responses for mechanical properties, and chemical compatibilities results.

Run	Component 1 A:Tio₂	Component 2 B:Al₂O₃	Factor 3 C:Dispersant	Factor 4 D: Mix	Factor 5 E:Formula	Adhesion	Wedge Bend	Acetic Acid*	Citric Acid*	Lactic Acid*	cystein chloride*	Pasteurization*
1	2	0	0	d	E	2.04	0.1	1	1	1	1	1
2	1	1	0.01	D	e	5	0.1	0	0	0	0	0
3	0	2	0	d	e	4.95	0.18	1	1	1	0	0
4	2	0	0.005	D	e	3.99	0.19	0	0	0	0	1
5	0	2	0	D	E	1.26	0.04	1	1	1	1	1
6	1	1	0.005	d	e	3.83	0.1	1	0	0	0	0
7	0	2	0.01	D	e	5	0.29	0	1	1	0	1
8	1	1	0.008	d	E	1.52	0.1	1	1	1	1	1
9	1	1	0.005	D	E	1.26	0.08	1	1	1	1	1
10	0	2	0.005	d	E	2.7	0.11	1	1	1	1	1
11	2	0	0	D	E	2.04	0.1	1	1	1	1	1
12	0	2	0.005	D	e	2.04	0.13	1	1	1	0	1
13	2	0	0.003	d	e	1.17	0.09	1	1	1	0	1
14	2	0	0.01	D	e	1.48	0.23	1	1	1	0	1
15	2	0	0.01	d	e	2.62	0.17	1	1	1	0	1
16	1	1	0.008	D	E	2.69	0.13	1	1	1	0	1
17	1	1	0	d	E	1.85	0	1	1	1	1	1
18	0	2	0.01	d	e	2.26	0.1	1	1	1	0	1
19	2	0	0.01	D	e	1.91	0.23	1	1	1	0	1
20	0	2	0.01	D	e	3.74	0.28	0	1	1	0	1
21	1	1	0.005	d	E	1.56	0	1	1	1	1	1
22	0	2	0	D	E	1	0.11	1	1	1	1	1
23	0	2	0	d	E	1.85	0.09	1	1	1	1	1
24	0	2	0	D	E	1.39	0.1	1	1	1	1	1
25	2	0	0.01	d	e	2.62	0.17	1	1	1	0	1
26	0	2	0	d	e	4.26	0.19	1	1	1	0	0
27	1	1	0.01	D	e	5	0.13	1	0	0	0	0
28	1.5	0.5	0.01	D	E	2.78	0.13	1	1	1	1	1
29	2	0	0.01	D	e	2.15	0.24	1	1	1	0	1
30	1.5	0.5	0.008	d	e	5	0.18	0	1	1	0	1
31	0	2	0.005	D	E	2.04	0.13	1	1	1	1	1
32	2	0	0	d	E	2.45	0.14	1	1	1	1	1
33	1	1	0.005	d	E	1.26	0.08	1	1	1	1	1
34	0	2	0	d	E	1.71	0.1	1	1	1	1	1

*0= not acceptable 1= acceptable

Table 3. The goodness of fitted models based on Analysis of variance (ANOVA).

Source	Sum of Squares	df	Mean Square	F Value	P-value
Adhesion					
Model	51.05	20	2.55	15.13	< 0.0001
Residual	2.19	13	0.17		
Lack of Fit	1.06	3	0.35	3.12	0.0748
R-Squared	0.96				
Adequacy Precision	12.62				
Standard Deviation	0.41				
Wedge Bend					
Model	0.12	11	0.011	11.36	< 0.0001
Residual	0.02	22	0.001		
Lack of Fit	0.02	12	0.002		
R-Squared	0.85				
Adequacy Precision	12.03				
Standard Deviation	0.03				

[a]degrees of freedom

Mechanical test results of nanocomposite

The results of adhesion, and wedge bend tests were detected based on Table 2. As shown in table 2, the highest amount of adhesion belonged to 5, 8, 9, 11, 12, 13, 14, 17, 19, 21, 22, 23, 24, 29, 31, 33 and 34 treatments. Moreover, the highest amount of wedge bend was allocated to 17 and 21 treatments.

Chemical compatibilities test results of nanocomposite

The results of chemical compatibility of nanocomposites under pasteurization and sterilization conditions are shown in Table 2. It can be seen that 1, 4, 5, 7, 8, 9, 10, 11, 12, 13, 14, 15, 16, 17, 18, 19, 20, 21, 22, 23, 24, 25, 28, 29, 30, 31, 32, 33 and 34 treatments had the chemical compatibilities against pasteurization condition. The chemical compatibilities of 1, 3, 5, 6, 8, 9, 10, 11, 12, 13, 14, 15, 16, 17, 18, 19, 21, 22, 23, 24, 25, 26, 27, 28, 29, 31, 32, 33, and 34 treatments against acetic acid were considered acceptable. The chemical compatibilities of 1, 3, 5, 7, 8, 9, 10, 11, 12, 13, 14, 15, 16, 17, 18, 19, 20, 21, 22, 23, 24, 25, 26, 28, 29, 30, 31, 32, 33 and 34 treatments against citric acid were considered acceptable. The chemical compatibilities of 1, 3, 5, 7, 8, 9, 10, 11, 12, 13, 14, 15, 16, 17, 18, 19, 20, 21, 22, 23, 24, 25, 26, 28, 29, 30, 31, 32, 33 and 34 treatments against lactic acid were considered acceptable. Moreover, the chemical compatibilities of 1, 5, 8, 9, 10, 11, 17, 21, 22, 23, 24, 28, 31, 32, 33 and 34 treatments against chloro-cysteine were considered acceptable.

Nanocomposite optimization results

As shown in Table 3, low and non-significant lack of fit, low standard deviation, low projected sum of squares, high R-squared, and high acceptable accuracy were used to determine the quality of fitted models. Quadratic and 2Fl models were shown to be the most effective models for adhesion response (Table 4). Thus, the wedge bend was fitted by quadratic and linear models. Based on Table 4, adhesion was significantly affected by the 2Fl term of the independent variable. Furthermore, the interaction between Al_2O_3 and formula (BE), and the interaction of TiO_2, Al_2O_3, and formula (ABE) were significantly affected by adhesion and wedge bend. The coefficient estimate for the response variables is shown in Table 5. It was confirmed that the interactions among TiO_2, Al_2O_3 and formula (ABE) were the most effective factors on adhesion properties. Hence, TiO_2 (A) and Al_2O_3 (B) were the main effective factors on the wedge bend.

Moreover, adhesion was positively affected by the major effects of TiO_2 (A), Al_2O_3 (B), and their interaction (AB). Whereas the principal detrimental effect on adhesion was caused by the interaction of TiO_2 (A), Al_2O_3 (B), dispersant (C), and formula (E). In general, by considering the absolute value of interactions, the effect of TiO_2 (A), Al_2O_3 (B), and their interactions (AB) were obvious. These results were evaluated further using two-component mix graphs.

Two component mix represents the effect of changing each mixture component while holding all others in a constant ratio. Fig. 1a-d indicated two component mix of adhesion. In Fig. 1a, by increasing TiO_2 and decreasing the Al_2O_3 in a fixed ratio of mix D, formula E, and dispersant 0.01 caused an increase in adhesion. This progress was

Table 4. Corresponding P-value for selected response variables.

Responses	Term																		
	AB	AC	AD	AE	BC	BD	BE	ABC	ABD	ABE	ACD	ACE	ADE	BCD	BCE	BDE	ABCD	ABCE	ABDE
adhesion	0.0003	0.0176	0.1534	0.9943	0.0010	0.2726	< 0.0001	0.0176	0.2781	< 0.0001	0.0050	0.5015	0.9563	0.6601	0.0008	0.9063	0.9179	0.0852	0.1889
Wedge Bend	0.0005	0.4949	0.0562	0.0053	0.0009	0.0199	< 0.0001	0.0944	0.9921	0.0776									

Table 5. The models used to show studied responses (y) as a function of independent variables (in terms of actual values).

Response	Model
Adhesion	R1= 2.62A+ 2.37B+ 4.19AB+ 0.46AC- 0.27AD+ 0.51BC+ 0.14BD+ 0.80BE- 2.24ABC+ 0.97ABD+ 6.14ABE- 0.53ACD- 0.12ACE- 0.054BCD+ 0.014BDE- 0.086ABCD- 1.74ABCE+ 1.16ABDE
Wedge Bend	R2= 0.15A+ 0.13B- 0.20AB-0.020AD+ 0.033AE + 0.034BC- 0.022BD+ 0.048BE+ 0.089ABC- 0.097ABE
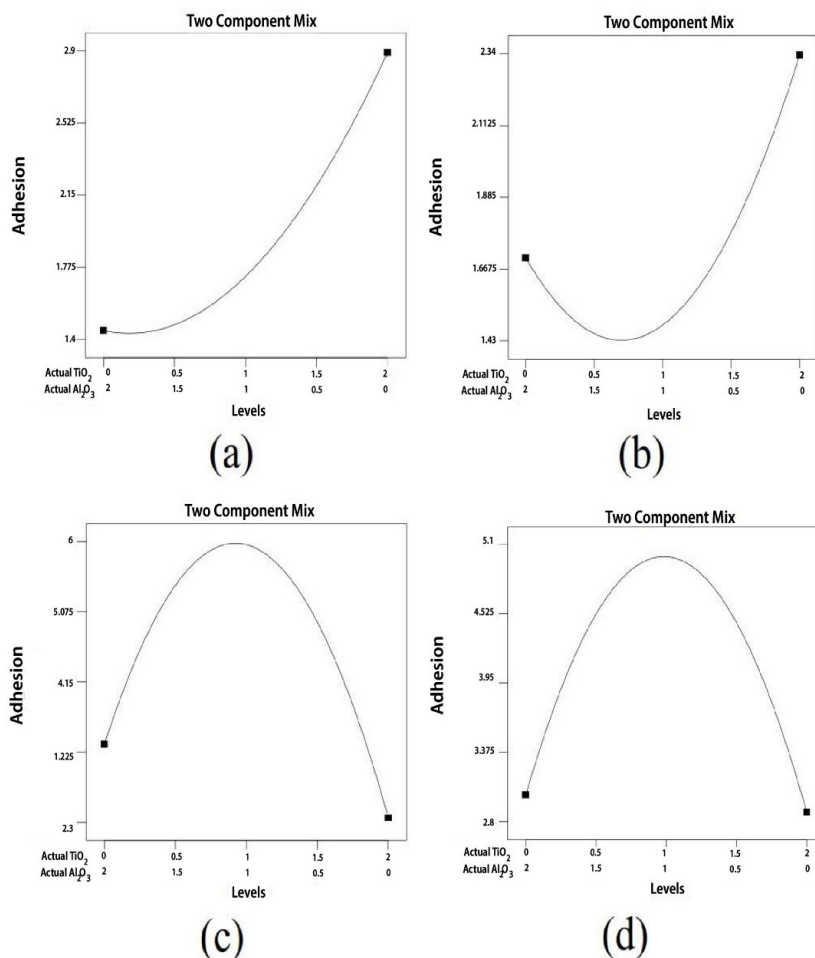
Fig. 1. Two component mix of adhesion with 0.01% dispersant, (a) in mix D and formula E, (b) in mix d and formula E, (c) in mix d and formula e, (d) in mix D and formula e.

undesirable. Although at this point, the score was raised, it was not in favor and caused the adhesion reduction. Since minimum adhesion was the main goal. In the mix d and formula E by increasing TiO$_2$ from 0 to 1%, and decreasing Al$_2$O$_3$ from 2 to 1% led to decrease the adhesion, and increasing TiO$_2$ from 1 to 2% and Al$_2$O$_3$ 1 to 0% led to increase it (Fig. 1b). While in constant ratio of mix d, formula e, and dispersant 0.01, by increasing TiO$_2$ from 0 to

1% and decreasing Al$_2$O$_3$ from 2 to 1% caused adhesion increase. Nguyen *et al*. [17] reported similar results when they added nano TiO$_2$ to epoxy resin. The increase in TiO$_2$ from 1 to 2% and the drop in Al$_2$O$_3$ from 1 to 0% resulted in a decrease in adhesion (Fig. 1c). This outcome matched that of combination D, formula e, and dispersant 0.01 just as well, as seen in Fig. 1d. The results showed that adding more nano Al$_2$O$_3$ increased the adherence
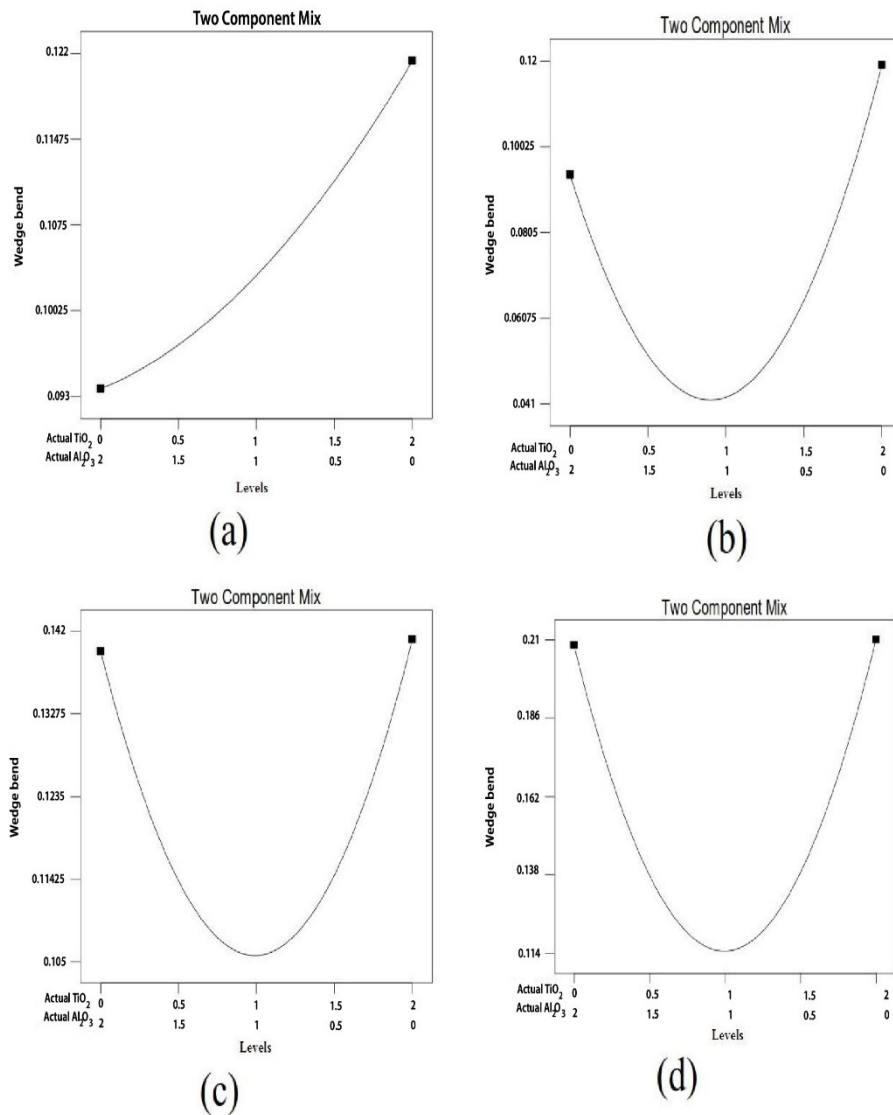
Fig. 2. Two component mix of wedge bend, (a) in mix D and formula E, (b) in mix d and formula E, (c) in mix d and formula e, (d) in mix D and formula e.

of epoxy, which is in line with Zhai *et al*.'s findings [27]. This may be accounted for by the influence of nanoparticles, which enhances the cured epoxy coating's adhesion to the substrate and modifies its mechanical characteristics. Furthermore, all results were the same and it can be seen that the dispersant had no significant effect on adhesion. It seems a low amount of consumed dispersant based on FDA regulations for food contact statutes at levels up to 0.5% by the weight of pigment can be effective in this regard.

The effect of two component mix on wedge bend was shown in Fig. 2a-d. In the constant ra-

tio of mix D, formula E and dispersant 0.01 the increase of TiO_2, and decrease of Al_2O_3 were in terms of the wedge bend enhancement (Fig. 2a). This result was observed by Khalil *et al*. [28] while, Al_2O_3 nanoparticles enhanced the mechanical properties of the epoxy matrix. The minimum wedge bend was the main goal. Flexibility was therefore not advantageous at this time. By increasing TiO_2 from 0% to 1% and decreasing Al_2O_3 from 2% to 1% wedge bend in mix d, formula E reduced. Following this, the result was incremental (Fig. 2b), with a rise in TiO_2 concentration and a fall in Al_2O_3 content. In mix D, formula e, dispersant 0.01, and
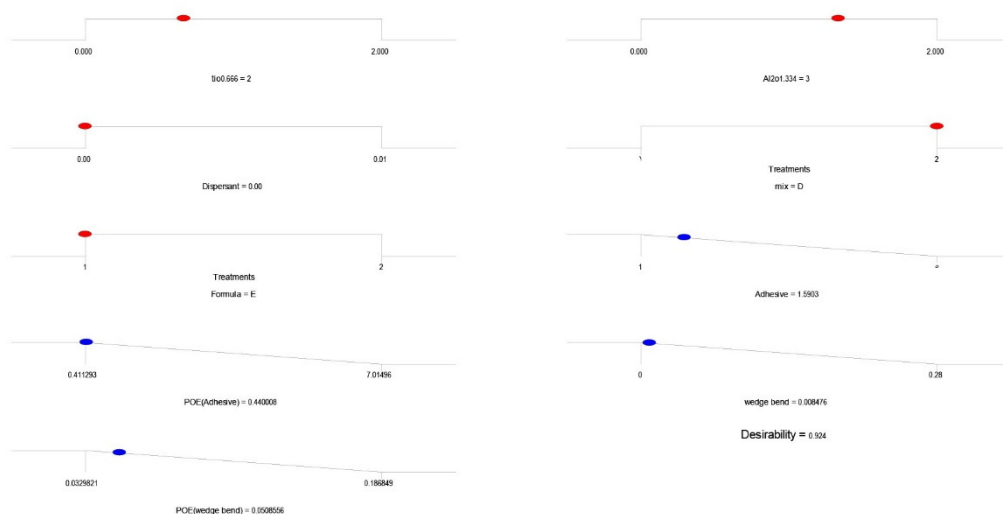
Fig. 3. The schematic representation of optimum values of factors, responses, and the corresponding levels.

Table 6. Experimental and predicted values of responses at optimized conditions.

Responses	Physical		Chemical					
	Adhesion (%)	Wedge bend	Acetic Acid	Citric Acid	Lactic Acid	cysteine chloride	Pasteurization	Desirability
Predicted value	[a]1.72± 0.27*	[b]0.093± 0.017*	-	-	-	-	-	0.924
Actual value	[a]2.56± 1.25*	[b]0.132± 0.064*	1	1	1	1	1	-

*Same alphabet shows no significant difference between predicted and actual based on paired t-test

mix D, formula e, the identical outcomes were seen (Fig. 2c-d). the same results were observed by Al-Turaif [16], they found that, the maximum flexural properties were found at a small percentage of 1% of TiO_2 particles. Wherein, Bittmann *et al*. [22] and Chatterjee and Islam [14] showed an improvement effect of TiO_2-nanoparticles on mechanical performance. This might be ascribed to some different conditions of mixture and formula type.

Furthermore, our findings showed that the dispersant had no discernible impact on the wedge bend characteristics. While the mechanical characteristics of the nanocomposite are being tuned, two response variables may be used to define the qualitative characteristics of the products. Since it's crucial to find the ideal criterion, they both need to be reduced. Therefore, the responses were considered in the range of studied levels. The optimum values were calculated by Derringer´s desirability function (Eq. 1):

$$D = \sqrt[m]{d^1 d^2 \dots d_m} \qquad (1)$$

Where m is the number of responses studied in the optimization process, and d is the individual desirability function of each response. Derringer´s desirability function (D) can take values from 0 to 1. A value of greater than 0.7 indicates a combination of the different criteria is matched in a global optimum [29].

Using the desirability function method, the following optimum condition was obtained: TiO_2= 0.66%, Al_2O_3= 1.33%, dispersant= 0%, mixing d (ultrasound) and formula E. The correlation of actual and predicted values was studied by paired t-test to certify the optimum point. The results indicated that, there was no significant different between predicted, and actual values (P >0.05). The aggregate attractiveness as well as the desirability for each piece and answer were both shown in Fig. 3's ramp view. Table 6 displays the anticipated value of replies under perfect circumstances. By considering high overall desirability functional and minimum propagation of error (POE) for each response, we represented optimal conditions as robust points. The value of 0.924 for desirability

denoted a valid optimum condition. These results suggested that a combined design was capable of the optimization of some mechanical properties of EP/ TiO_2/ Al_2O_3 nanocomposite.

To study the PLS-DA, 35 samples were selected. These samples were obtained using a D-optimal combined design (34 runs), and one sample was selected and formulated by optimization process (named 35).

PLS-DA is one of the classification methods which search for latent variables with a maximum covariance. A classification model can be the best way to study the qualitative model response. For example, each definable object can be associated with a qualitative binary response (yes/no). Furthermore, the classification model can be an appropriate way to outcome process (acceptable or not acceptable) [30]. The data were divided into categories using the PLS-DA modeling procedure. A good PLS-DA model requires cross-validation and the right preprocessing techniques. Data was automatically scaled and cross-validated using the leave one out approach prior to PLS-DA modeling. PLS-DA model analysis yielded two latent variables which contribute about 94.32% of the total variance in the data. The first latent variable LV1 indicated 74.02% and the second latent variable LV2 showed 20.3% of the total variance. Fig. 4 showed score plots for two latent variables of the PLS-DA model and illustrate that sample number 35 (opti-

mized sample) was placed in +LV1 and +LV2, where samples number of 2, 3, 4, 6, 7, 20, 26, 27, and 30 were settled in –LV1 and –LV2, and other samples in –LV1 and +LV2. No samples were inserted into the +LV1 and -LV2, as shown in Fig. 4. Sample number 35 (the optimized sample), when compared to other samples, demonstrated strong discrimination, according to the score plots for two latent variables. Variable importance in the projection VIP scores applied to identify the variables that were the most significant factor for the discrimination. VIP scores were greater than one used as a criterion to identify the most significant variables. In Fig. 5, the values of the VIP score for the mechanical and chemical variables are shown. It can be observed that the wedge bend, adhesion and pasteurization condition were the most significant variables by 2.73, 2.02, and 1.38, respectively.

Optimized nanocomposite Field Emission Scanning Electron Microscope (FESEM) results

Fig. 6 (a, b) displays the surface morphology of the neat epoxy and Fig. 6 (c, d) displays the surface morphology of the cured nanocomposites as determined by FE-SEM with EDX element mapping. The nanoparticles' FESEM picture showed that both their size and shape were uniformly nanoscale. These photos demonstrated that the average particle size was roughly 90 nm under ideal circumstances. Based on Fig. 6 (d), the EDX graph
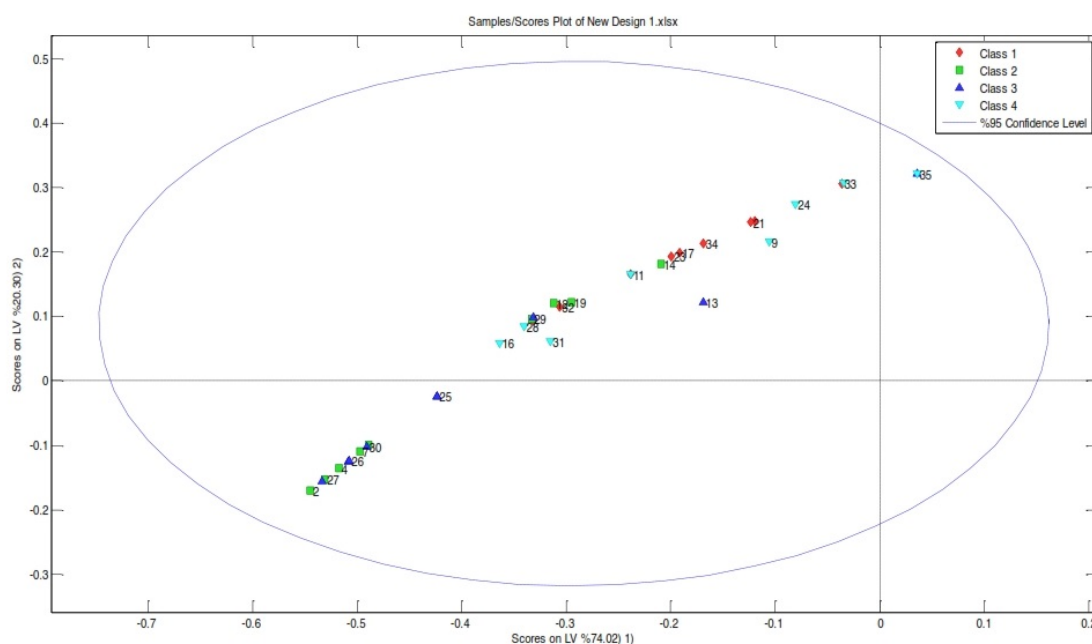

Fig. 4. PLS-DA scores plot (LV1 vs., LV2) in the analysis of selected runs and optimum point.
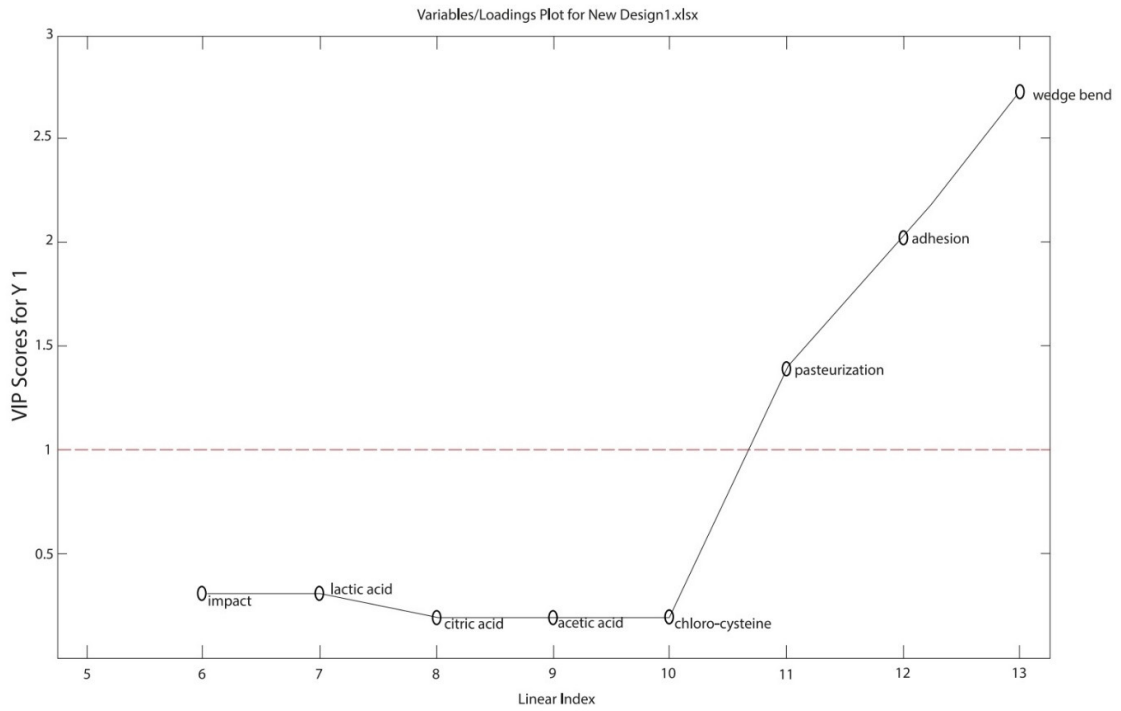
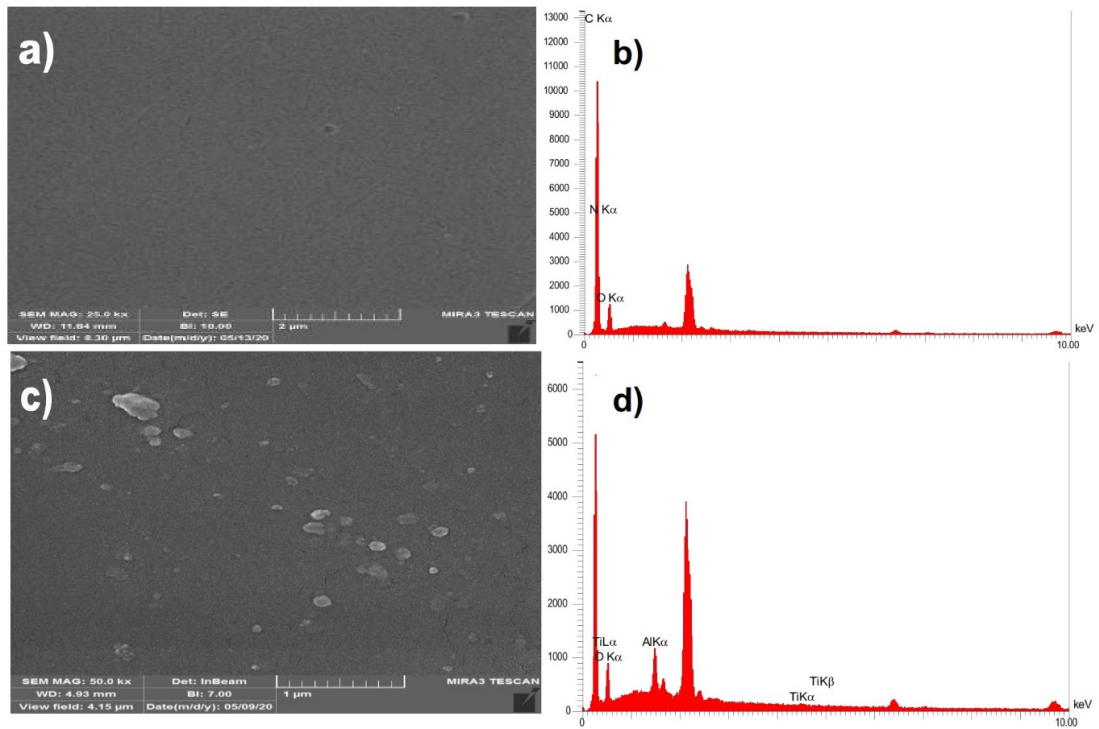Fig. 5. VIP scores of variables in the PLS-DA model.

Fig. 6. FESEM image of (a) neat epoxy, (b) EDX spectra of neat epoxy, (c) FESEM image of epoxy/TiO_2/Al_2O_3 nanocomposite, and (d) EDX spectra of epoxy/TiO_2/Al_2O_3 nanocomposite.
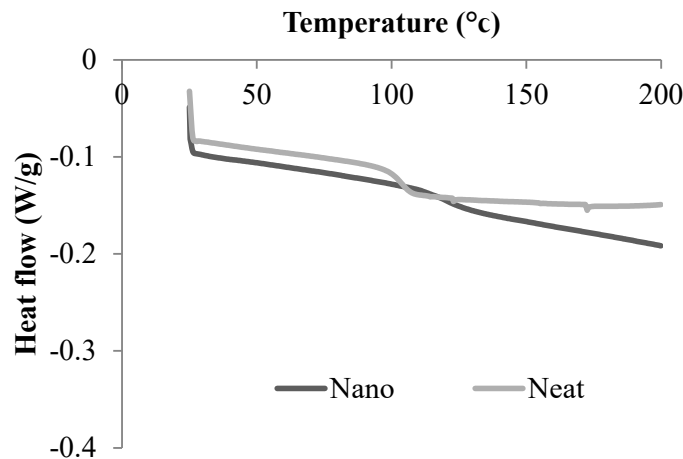
Temperature (°c)

Fig. 7. Glass transition temperature of neat epoxy and epoxy/TiO$_2$/Al$_2$O$_3$ nanocomposite.

only showed the presence of Al, Ti and O (50.33, 3.42, and 46.25W%, respectively) in the nanocomposite.

Optimized nanocomposite Differential Scanning Calorimeter (DSC) results

The results of measuring glass transition temperature by applying a differential scanning calorimeter are shown in Fig. 7 The original epoxy resins and nanocomposite glass transition temperature were measured using DSC which were 103.52 °C and 120.98 °C, respectively. Our findings were similar to Ben Samuel *et al.* [31] reports. They reported epoxy resins including nano-silica particles (2 v/w%) had higher glass transition than epoxy resin. Moreover, the *T*g value of nano epoxy composite 1% and nano TiO$_2$ was higher than (79 to 84 °C) that of neat epoxy [32]. The same results were obtained by adding 0.5% of nano Al$_2$O$_3$ to epoxy which caused *T*g to increase from 191.7 to 205.6 °C [33].

All cross-linking density [34], free volume [35, 36], and the nano surface adhesion and epoxy interfacial layer [17, 18] were affected by the glass transition temperature.

Cross-linking density has a significant role to regulate the glass transition temperature for a typical thermosetting polymer setting system. Since cross-linking density and the glass transition temperature are intimately correlated, raising the glass transition temperature raises the cross-linking density [17]. If the nanoparticles are distributed properly throughout the composite, such as by the polar force of the nanoparticles and the mas-

sive van der Waals bond in the nanocomposite, the crosslinking formation of the nanocomposite in the multilayer bond between the resin and the hardener will be increased compared to epoxy. This phenomenon can be related to use of free volume in the composite structure. In a polymer matrix, increasing the crosslinking complication reduces the specific free volume. Consequently, molecular motion requires more energy to rotate. Therefore, the *T*g value can be increased [37, 38]. Evora and Shukla showed that the restriction of resin networks based on the decrease in particle sizes, and glass transition temperature extremely could increase for the small particles [39]. Furthermore, a certain weak dispersion caused a decrease in the glass transition temperature consistent by increasing the accumulation of particles [14, 40]. If there is insufficient cohesion between the nanoparticles and the matrix, the crosslinking and glass transition temperature may be attenuated. The glass transition temperature may be decreased due to the tension concentration surrounding cohesive nanofillers [41]. Furthermore, the interactions between the polymer chains and the surface of high-charge nanoparticles lead to the formation of a polymer nanolayer that is close to the surface of nanoparticle, and it is the interfacial nanolayer which appoints glass transition temperature [17, 28, 42].

Optimized nanocomposite Dynamic Mechanic Analysis (DMA) results

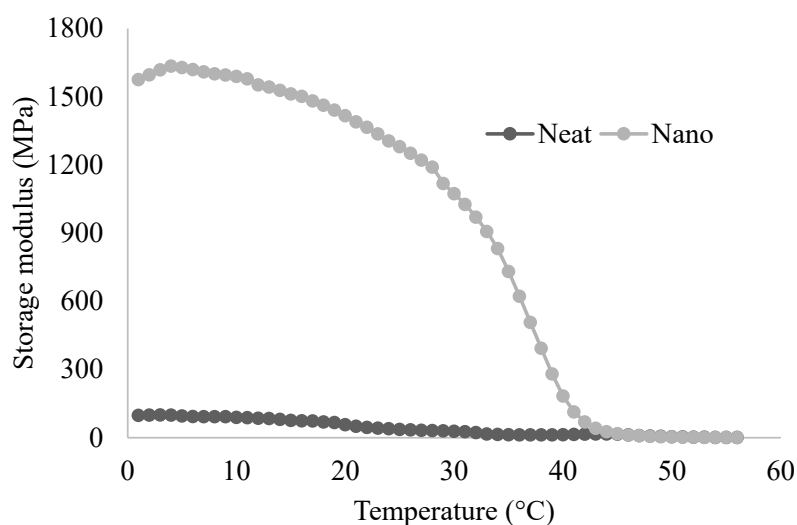The storage modulus of neat epoxy and the nanocomposites measured using DMA are indi-

Fig. 8. DMA results of neat and nanophase epoxy.

cated in Fig. 8. Viscoelastic responses of material were perceived from DMA analysis. Features like storage modulus were measured under dynamic loading conditions in a temperature range. The storage modulus (E) indicates the stiffness of viscoelastic material which is known as the energy stored in the load cycle.

DMA plots of storage modulus in different ranges of temperatures are illustrated in Fig. 8. It was found that the storage modulus changed as a function of temperature and nanoparticle concentration in unmodified and nanocomposites with and without nanoparticles. The values of E reduced with rising the temperature, which indicated the material state shifts from glass to rubber. However, when the epoxy was strengthened by the addition of nano-sized TiO_2 and Al_2O_3 particles, E values increased, demonstrating the reinforcing impact of the nanoparticles. The storage modulus was considerably enhanced when nanoparticles were present. Similar results were seen in other nanocomposites [28, 43] which showed that, adding 2 wt% of the nano TiO_2 and Al_2O_3 could significantly increase the storage modulus at 31°C. The same result was observed in a research titled the improvement of Storage Modulus by loading nano alumina to the epoxy [44]. Furthermore, the storage modulus of reinforced epoxy composites with 4 wt% of the nano TiO_2 showed the maximum enhancement (32.8%) compared to neat epoxy [45]. The nanocomposite under loading nano TiO_2 and Al_2O_3 had more surface areas and enhance

more interfacial interactions with the matrix. Therefore, the mobility of polymer chains can be reduced, and stress transfer at the interface can be improved. According to a widely accepted theory [44, 46], the enhancement in the mechanical and dynamic properties of reinforced composites can be attributed to the expansion of a chemically bonded system that is more rigid and firmer.

CONCLUSIONS

A combined design was used to optimize some mechanical properties of EP/ TiO_2/ Al_2O_3 nanocomposite. 2FI and quadratic models were found the best models for adhesion, so the wedge bend was fitted by linear and quadratic models. The result confirmed that TiO_2, Al_2O_3 and formula (ABE) were the most effective factors in the adhesion and wedge bend. Moreover, it was concluded that the best mechanical properties can be achieved at an optimal condition (TiO_2 0.66%, Al_2O_3 1.33%, dispersant 0.000017%, mixing d (ultrasound), and formula E 0.924 desirability). PLS-DA analysis indicated the optimum point had discrimination in comparison with other samples. By VIP scores, the distance, wedge bend, adhesion, and thermal treatment were the most significant variables. The analysis of variance (ANOVA) on the models revealed that the predicted model was significant (P < 0.05) and its lack of fit test was not significant. A high coefficient of determination, and high enough accuracy indicated a good fit of the predicted model to the experimental data. Thus, the model's

high corrected coefficient of determination and sufficient accuracy demonstrated its applicability for forecasting experimental data. A very low coefficient of variation clearly showed that obtained experimental data had high reproducibility and reliability. Based on FESEM and EDX images, the epoxy/TiO_2/Al_2O_3 nanocomposite had a uniform particle distribution size. The DSC analysis showed the TiO_2 (0.66%), and Al_2O_3 (1.33%) nanoparticles loading and the glass transition temperature (about 17.46°C), and considerable improvement in thermal stability of epoxy/TiO_2/Al_2O_3 nanocomposite. This improvement was assigned to the homogeneous dispersion of nanoparticles in the epoxy matrix. DMA analysis showed an increase in the storage modulus of the epoxy/TiO_2/Al_2O_3 nanocomposite which was attributed to the improvement of elasticity. The epoxy nanocomposite showed greater thermal stability and elasticity than the control sample. Utilizing nanotechnology, it will be possible in the future to create products with superior functional properties.

ACKNOWLEDGMENT

CONFLICT OF INTEREST

The authors confirm that there is no conflict of interest in this article content.

REFERENCES

[1] Jin F. L., Li X., Park S. J., (2015), Synthesis and application of epoxy resins: A review. J. Ind. Eng. Chem. 29: 1-11. https://doi.org/10.1016/j.jiec.2015.03.026

[2] Xiong Y., Jiang Z., Xie Y., Zhang X., Xu W., (2013), Development of a DOPO-containing melamine epoxy hardeners and its thermal and flame-retardant properties of cured products. J. Appl. Polym. Sci. 127: 4352-4358. https://doi.org/10.1002/app.37635

[3] Jiang W., Zhou G., Wang C., Xue Y., Niu, C., (2021), Synthesis and self-healing properties of composite microcapsule based on sodium alginate/melamine-phenol-formaldehyde resin. Constr. Build. Mater. 271: 121541-121544. https://doi.org/10.1016/j.conbuildmat.2020.121541

[4] Qiao W., Li S., Guo G., Han S., Ren S., Ma Y., (2015), Synthesis and characterization of phenol-formaldehyde resin using enzymatic hydrolysis lignin. J. Ind. Eng. Chem. 21: 1417-1422. https://doi.org/10.1016/j.jiec.2014.06.016

[5] Kopal I., Vršková J., Labaj I., Ondrušová D., Hybler P., Harničárová M., Kušnerová M., (2018), The effect of high-energy ionizing radiation on the mechanical properties of a melamine resin, phenol-formaldehyde resin, and nitrile rubber blend. Materials. 11: 2405-2408. https://doi.org/10.3390/ma11122405

[6] Rahimi M., Sadeghi B., Kargar Razi M., (2021), Influence of Al2O3 additive on mechanical properties of wollastonite glass-ceramics. ADMT Journal. 14: 25-33.

[7] Thirumalai A., Harini K., Pallavi P., Gowtham P., Girigoswami K., Girigoswami A., (2023), Nanotechnology driven improvement of smart food packaging. Mater. Res. Innov. 27: 223-232. https://doi.org/10.1080/14328917.2022.2114667

[8] Shi X. H., Li X. L., Li Y. M., Li Z., Wang D. Y., (2022), Flame-retardant strategy and mechanism of fiber reinforced polymeric composite: A review. Compos. Part B. Eng. 109663. https://doi.org/10.1016/j.compositesb.2022.109663

[9] Montazeri A., Montazeri N., Pourshamsian K., Tcharkhtchi A., (2011), The effect of sonication time and dispersing medium on the mechanical properties of multiwalled carbon nanotube (MWCNT)/epoxy composite. Int. J. Polym. Analys. Charact. 16: 465-476. https://doi.org/10.1080/1023666X.2011.600517

[10] Pötschke P., Bhattacharyya A. R., Janke A., Goering H., (2003), Melt mixing of polycarbonate/multi-wall carbon nanotube composites. Compos. Interf. 10: 389-404. https://doi.org/10.1163/156855403771953650

[11] Ashjari M., Mahdavian A. R., Ebrahimi N. G., Mosleh Y., (2010), Efficient dispersion of magnetite nanoparticles in the polyurethane matrix through solution mixing and investigation of the nanocomposite properties. J. Inorg. Organomet. Polym. Mater. 20: 213-219. https://doi.org/10.1007/s10904-010-9337-x

[12] Rajaraman T. S., Gandhi V. G., Nguyen V. H., Parikh S. P., (2023), Aluminium foil-assisted NaBH4 reduced TiO2 with surface defects for photocatalytic degradation of toxic fuchsin basic dye. Appl. Nanosc. 13: 3925-3944. https://doi.org/10.1007/s13204-022-02628-x

[13] Ramanathan T., Abdala A. A., Stankovich S., Dikin D. A., Herrera-Alonso M., Piner R. D., Brinson L. C., (2008), Functionalized graphene sheets for polymer nanocomposites. Nat. Nanotechnol. 3: 327-331. https://doi.org/10.1038/nnano.2008.96

[14] Chatterjee A., Muhammad S. I., (2008), Fabrication and characterization of TiO2-epoxy nanocomposite. Mater. Sci. Eng. A. 487: 574-585. https://doi.org/10.1016/j.msea.2007.11.052

[15] Mousavi S. R., Estaji S., Paydayesh A., Arjmand M., Jafari S. H., Nouranian S., Khonakdar H. A., (2022), A review of recent progress in improving the fracture toughness of epoxy based composites using carbonaceous nanofillers. Polym. Compos. 43: 1871-1886. https://doi.org/10.1002/pc.26518

[16] Al-Turaif H. A., (2010), Effect of nano TiO2 particle size on mechanical properties of cured epoxy resin. Prog. Org. Coat. 69: 241-246. https://doi.org/10.1016/j.porgcoat.2010.05.011

[17] Nguyen T. A., Nguyen T. V., Thai H., Shi X., (2016), Effect of nanoparticles on the thermal and mechanical properties of epoxy coatings. J. Nanosci. Nanotechnol. 16: 9874-9881. https://doi.org/10.1166/jnn.2016.12162

[18] Jiang T., Kuila T., Kim N. H., Lee J. H., (2014), Effects of surface-modified silica nanoparticles attached graphene oxide using isocyanate-terminated flexible polymer chains

on the mechanical properties of epoxy composites. J. Mater. Chem. A. 2: 10557-10567. https://doi.org/10.1039/C4TA00584H

[19] Majdzadeh-Ardakani K., Navarchian A. H., Sadeghi F., (2010), Optimization of mechanical properties of thermoplastic starch/clay nanocomposites. Carbohydr. Polym. 79: 547-554. https://doi.org/10.1016/j.carbpol.2009.09.001

[20] Nguyen T. A., Nguyen Q. T., Bach T. P., (2019), Mechanical properties and flame retardancy of epoxy resin/nanoclay/multiwalled carbon nanotube nanocomposites. J. Chem. 2019: Article ID 3105205 | https://doi.org/10.1155/2019/3105205

[21] Keyoonwong W., Guo Y., Kubouchi M., Aoki S., Sakai T., (2012), Corrosion behavior of three nanoclay dispersion methods of epoxy/organoclay nanocomposites. Int. J. Corros. 2012: Article ID 924283 | https://doi.org/10.1155/2012/924283

[22] Bittmann B., Haupert F., Schlarb A. K., (2012), Preparation of TiO2 epoxy nanocomposites by ultrasonic dispersion and resulting properties. J. Appl. Polym. Sci. 124: 1906-1911. https://doi.org/10.1002/app.34493

[23] Duarte B., Mamede R., Carreiras J., Duarte I. A., Caçador I., Reis-Santos P., Fonseca V. F., (2022), Harnessing the full power of chemometric-based analysis of total reflection X-ray fluorescence spectral data to boost the identification of seafood provenance and fishing areas. Foods 11: 2699-2703. https://doi.org/10.3390/foods11172699

[24] de Queiroz Baddini A. L., de Paula Santos J. L. V., Tavares R. R., de Paula L. S., da Costa Araújo Filho H., Freitas R. P., (2022), PLS-DA and data fusion of visible reflectance, XRF and FTIR spectroscopy in the classification of mixed historical pigments. Spectrochim. Acta A Mol. Biomol. Spectrosc. 265: 120384-120387. https://doi.org/10.1016/j.saa.2021.120384

[25] Della Gatta G., Richardson M. J., Sarge S. M., Stølen S., (2006), Standards, calibration, and guidelines in microcalorimetry. Part 2. Calibration standards for differential scanning calorimetry*(IUPAC Technical Report). Pure Appl. Chem. 78: 1455-1476. https://doi.org/10.1351/pac200678071455

[26] Maity T., Samanta B. C., Dalai S., Banthia A. K., (2007), Curing study of epoxy resin by new aromatic amine functional curing agents along with mechanical and thermal evaluation. Mater. Sci. Eng. A. 464: 38-46. https://doi.org/10.1016/j.msea.2007.01.128

[27] Zhai L. L., Ling G. P., Wang Y. W., (2008), Effect of nano-Al2O3 on adhesion strength of epoxy adhesive and steel. Int. J. Adhes. Adhes. 28: 23-28. https://doi.org/10.1016/j.ijadhadh.2007.03.005

[28] Khalil N. Z., Johanne M. F., Ishak M., (2019), Influence of Al2O3 nanoreinforcement on the adhesion and thermomechanical properties for epoxy adhesive. Compos. Part B Eng. 172: 9-15. https://doi.org/10.1016/j.compositesb.2019.05.007

[29] Bezerra M. A., Santelli R. E., Oliveira E. P., Villar L. S., Escaleira L. A., (2008), Response surface methodology (RSM) as a tool for optimization in analytical chemistry. Talanta. 76: 965-977. https://doi.org/10.1016/j.talanta.2008.05.019

[30] Botelho B. G., Reis N., Oliveira L. S., Sena M. M., (2015), Development and analytical validation of a screening method for simultaneous detection of five adulterants in raw milk using mid-infrared spectroscopy and PLS-DA. Food Chem. 181: 31-37. https://doi.org/10.1016/j.foodchem.2015.02.077

[31] Ben Samuel J., Julyes Jaisingh S., Sivakumar K., Mayakannan A. V., Arunprakash V. R., (2021), Visco-elastic, thermal, antimicrobial and dielectric behaviour of areca fibre-reinforced nano-silica and neem oil-toughened epoxy resin bio composite. Silicon. 13: 1703-1712. https://doi.org/10.1007/s12633-020-00569-0

[32] Radoman T. S., Džunuzović J. V., Grgur B. N., Gvozdenović M. M., Jugović B. Z., Miličević D. S., Džunuzović E. S., (2016), Improvement of the epoxy coating properties by incorporation of polyaniline surface treated TiO2 nanoparticles previously modified with vitamin B6. Prog. Org. Coat. 99: 346-355. https://doi.org/10.1016/j.porgcoat.2016.06.014

[33] Yu Z. Q., You S. L., Yang Z. G., Baier H., (2011), Effect of surface functional modification of nano-alumina particles on thermal and mechanical properties of epoxy nanocomposites. Adv. Compos. Mater. 20: 487-502. https://doi.org/10.1163/092430411X579104

[34] Vryonis O., Virtanen S. T. H., Andritsch T., Vaughan A. S., Lewin P. L., (2019), Understanding the cross-linking reactions in highly oxidized graphene/epoxy nanocomposite systems. J. Mater. Sci. 54: 3035-3051. https://doi.org/10.1007/s10853-018-3076-8

[35] Yao X. F., Yeh H. Y., Zhou D., Zhang Y. H., (2006), The structural characterization and properties of SiO2-epoxy nanocomposites. J. Compos. Mater. 40: 371-381. https://doi.org/10.1177/0021998305055193

[36] Mohammadi M., Davoodi J., Javanbakht M., Rezaei H., (2018), Glass transition temperature of PMMA/modified alumina nanocomposite: Molecular dynamic study. Mater. Res. Express 6: 035309. https://doi.org/10.1088/2053-1591/aaf6d5

[37] Sharma S. K., Sudarshan K., Sahu M., Pujari P. K., (2016), Investigation of free volume characteristics of the interfacial layer in poly (methyl methacrylate)-alumina nanocomposite and its role in thermal behaviour. RSC Adv. 6: 67997-68004. https://doi.org/10.1039/C6RA07051E

[38] Wang Z., Pang H., Li G., Zhang Z., (2006), Glass transition and free volume of high impact polystyrene/TiO2 nanocomposites determined by dilatometry. J. Macromol. Sci. B. 45: 689-697. https://doi.org/10.1080/00222340600890497

[39] Evora Victor M. F., Arun S., (2003), Fabrication, characterization, and dynamic behavior of polyester/TiO2 nanocomposites. Mater. Sci. Eng. A. 361: 358-366. https://doi.org/10.1016/S0921-5093(03)00536-7

[40] Natarajan B., Li Y., Deng H., Brinson L. C., Schadler L. S., (2013), Effect of interfacial energetics on dispersion and glass transition temperature in polymer nanocomposites. Macromolecules. 46: 2833-2841. https://doi.org/10.1021/ma302281b

[41] Aradhana R., Mohanty S., Nayak S. K., (2018), Comparison of mechanical, electrical and thermal properties in graphene oxide and reduced graphene oxide filled epoxy nanocomposite adhesives. Polymer. 141: 109-123. https://doi.org/10.1016/j.polymer.2018.03.005

[42] Sunday D. F., David L. G., (2015), Thermal and rheological behavior of polymer grafted nanoparticles. Macromolecules. 48: 8651-8659. https://doi.org/10.1021/acs.macromol.5b00987

[43] Cao Y. M., Sun J., Yu D. H., (2002), Preparation and properties of nano-Al2O3 particles/polyester/epoxy resin ternary composites. J. Appl. Polym. Sci. 83: 70-77. https://doi.org/10.1002/app.10020

[44] Kumar A., Sharma K., Dixit A. R., (2019), A review of the

mechanical and thermal properties of graphene and its hybrid polymer nanocomposites for structural applications. J. Mater. Sci. 54: 5992-6026. https://doi.org/10.1007/s10853-018-03244-3

[45] Singh S. K., Singh S., Kumar A., Jain A., (2017), Thermo-mechanical behavior of TiO2 dispersed epoxy composites. Eng. Fract. Mech. 184: 241-248. https://doi.org/10.1016/j.engfracmech.2017.09.005

[46] Moon R. J., Martini A., Nairn J., Simonsen J., Youngblood J., (2011), Cellulose nanomaterials review: Structure, properties and nanocomposites. Chem. Soc. Rev. 40: 3941-3994. https://doi.org/10.1039/c0cs00108b